Report Title: Materials System for Intermediate Temperature Solid Oxide Fuel Cell

Type of Report: Annual Technical Progress report

Reporting Period Start Date: 9/26/03

Reporting Period End Date: 9/25/04

Principal Author(s): Professors Uday B. Pal and Srikanth Gopalan

Dated: January 24, 2005

DOE Award Number: DE-FG26-02NG41539

Department of Manufacturing
15 St. Mary's Street
Boston University, MA 02446

Abstract

AC complex impedance spectroscopy studies were conducted between 600-800°C on symmetrical cells that employed strontium-and-magnesium-doped lanthanum gallate electrolyte, $La_{0.9}Sr_{0.1}Ga_{0.8}Mg_{0.2}O_3$ (LSGM). The objective of the study was to identify the materials system for fabrication and evaluation of intermediate temperature (600-800°C) solid oxide fuel cells (SOFCs). The slurry-coated electrode materials had fine porosity to enhance catalytic activity. Cathode materials investigated include $La_{1-x}Sr_xMnO_3$ (LSM), LSCF ($La_{1-x}Sr_xCo_yFe_{1-y}O_3$), a two-phase particulate composite consisting of LSM-doped-lanthanum gallate (LSGM), and LSCF-LSGM. The anode materials were Ni-$Ce_{0.85}Gd_{0.15}O_2$ (Ni-GDC) and Ni-$Ce_{0.6}La_{0.4}O_2$ (Ni-LDC) composites. Experiments conducted with the anode materials investigated the effect of having a barrier layer of GDC or LDC in between the LSGM electrolyte and the Ni-composite anode to prevent adverse reaction of the Ni with lanthanum in LSGM. For proper interpretation of the beneficial effects of the barrier layer, similar measurements were performed without the barrier layer. The ohmic and the polarization resistances of the system were obtained over time as a function of temperature (600-800°C), firing temperature, thickness, and the composition of the electrodes. The study revealed important details pertaining to the ohmic and the polarization resistances of the electrode as they relate to stability and the charge-transfer reactions that occur in such electrode structures.

Table of Contents

List of Graphical Materials

Introduction

Solid oxide fuel cells (SOFCs) represent one of the most environmentally clean and versatile means of efficiently converting chemical energy to electrical energy from a wide variety of fossil fuels. Despite their many advantages, SOFC power systems are not yet cost-effective to merit large-scale deployment in the power generation industry. Of the approaches currently being investigated to decrease the cost of SOFCs, improving power density while decreasing operating temperature is perhaps the most promising option. However, decreasing operating temperature has the effect of increasing all types of performance losses in the cell. Thus the simultaneous goals of improving power density while lowering the operating temperature are at odds with each other. Therefore, the focus of recent research is aimed at development of more active electrodes and more conductive electrolyte materials that can efficiently operate at lower temperatures (600-800^{o}C).

The material property requirements for SOFCs are quite stringent and well established [1-3]. Sr and Mg doped $LaGaO_3$ (LSGM) is currently considered as one of the most promising electrolyte materials for intermediate-temperature SOFCs [4-5]. It has significantly higher oxygen-ion conductivity than conventional yttria-stabilized zirconia (YSZ) between (600-800^{o}C) and negligible electronic conductivity over a wide range of oxygen partial pressures employed under SOFC operating conditions.

The electrode kinetics has a strong exponential dependence on temperature and so lower operating temperatures would result in significant polarization losses, particularly charge-transfer polarization losses at the electrode-electrolyte interfaces. This will drastically reduce the cell efficiency [2]. Hence, if the operating temperature of the SOFC is to be lowered, an entirely new material system for the electrodes is needed as well. This report contains the results of several prospective anode and cathode materials for application in Intermediate-Temperature (600-800^{o}C) SOFCs employing LSGM electrolyte. Cathode materials that are studied include state-of-the-art electrode material for YSZ electrolyte SOFCs (Sr-doped lanthanum manganite or LSM), Sr-doped lanthanum cobalt iron oxide (LSCF), porous composite electrodes comprising LSM-LSGM and LSCF-LSGM compositions. The choice of anode materials was based on Ni-doped ceria composite electrodes. Nickel is a well-known SOFC anode material, and acts as the fuel side electrocatalyst and current collector. Usually the SOFC anodes are prepared by mixing and sintering NiO and an oxygen-ion-conducting oxide in air, followed by reducing the NiO to Ni under reducing conditions. Use of lanthanum or gadolinium doped ceria as the oxygen-ion-conducting oxide in the anode would buffer the thermal expansion mismatch between the anode and the electrolyte and also result in lowering the charge-transfer polarization due to its mixed-conducting property [5-6]; La-or-Gd-doped ceria conducts both oxygen ions and electrons. It has been observed that the Ni phase in the anode reacts with the perovskite LSGM phase forming an insulating lanthanum nickelate phase and this also causes the ohmic and anodic polarization resistance to increase with time. In response to this observation the concept of applying a doped (lanthanum or gadolinium) ceria barrier or buffer layer to prevent direct contact and reaction of Ni with the LSGM electrolyte is also investigated. Since the doped ceria has sufficiently high oxygen-ion conductivity and the buffer layer will be thin (< 5μm), it is not expected to increase the ohmic polarization resistance of the cell. The purpose of this work is to identify a possible material system and structure for the intermediate-temperature SOFC.

Executive Summary

The objective of the proposed research is to investigate a materials system for intermediate temperature solid oxide fuel cell that is capable of operating between 500-700^{0}C with a power density greater than 0.6W/cm^2 at 0.7V. The electrolyte, anode, and cathode materials in the SOFC system being investigated are based on lanthanum gallate ($La_{1-x}Sr_xGa_{1-y}Mg_yO_{3-\delta}$ or LSGM), nickel-ceria ($Ce_{0.9}Y_{0.1}O_{2-x}$) cermet, and LSGM-lanthanum cobaltite ($La_{0.8}Sr_{0.2}CoO_3$, or LSC) composite, respectively. These material choices are based on their property information available in the literature, which indicate that they meet the operational requirements of the intermediate-temperature SOFC.

Interfacial polarizations of the candidate electrodes for the $La_{0.9}Sr_{0.1}Ga_{0.8}Mg_{0.2}O_3$ (LSGM) electrolyte have been investigated by Impedance spectroscopy technique.

Several cathode materials have been studied for application in Intermediate Temperature (IT)-SOFCs including the state-of-the-art cathode material, LSM, strontium doped lanthanum cobalt iron oxide (LSCF), porous composite electrodes comprising LSM-LSGM and LSCF-LSGM compositions. The polarization resistances of the cathode materials were measured using impedance spectroscopy on symmetric cells as a function of temperature. Based on these measurements we have identified a 50 vol% porous composite of LSCF and LSGM as the best cathode material. The LSCF-LSGM composite cathode has a polarization resistance that is orders of magnitude lower than both conventional LSM and composite LSM-LSGM cathodes, and also slightly lower than the single phase LSCF cathode. Considering the thermal expansion coefficient (TEC) mismatch between the LSCF cathode and LSGM electrolyte, the LSCF-LSGM composite is also preferred over single phase LSCF. Investigations of IT-SOFC cathode materials have also revealed a dependence of polarization resistance on thickness. The polarization of the cathode layer initially decreases sharply with increasing electrode thickness and then levels off asymptotically. The initial decrease of the cathode polarization resistance can be rationalized on the premise that increasing the electrode thickness results in an increase in the number of electrochemical reaction sites, i.e. total three-phase boundary length in the case of composite cathodes, or total pore area in the case of mixed ionic-electronic conductors. The subsequent leveling off of the polarization resistance is due to the fact that above a certain critical electrode thickness the migration of the oxygen ions from the reaction sites to the electrode/electrolyte interface become rate controlling. Thus, there is a certain critical thickness beyond which the cathodic polarization resistance shows no further decrease with increasing thickness. This critical electrode thickness is a strong function of the microstructure (grain size) and porosity, i.e. finer the microstructure and finer the porosity, smaller the critical thickness. The fabricated cathodes typically have 1μm average grain size and 25% porosity. From our measurements it is clear that a cathode thickness of 40 μm is sufficient to minimize the polarization resistance. The anode materials investigated were Ni-Gadolinium and Ni-Lanthanum doped Ceria (Ni-GDC and Ni-LDC). It was observed that the LSGM electrolyte reacts with the Ni during processing and also at the operating temperature and increases the polarization resistance. A dense buffer layer of LDC between the LSGM electrolyte and the composite anode prevents this interaction and a much lower electrode polarization is observed. Anode-supported planer cells are being fabricated and evaluated in terms of its I-V characteristics and component stability.

Experimental

Powder synthesis: Electrolyte powders of the composition $La_{0.9}Sr_{0.1}Ga_{0.8}Mg_{0.2}O_3$ (LSGM) were synthesized by mixing and ball-milling high purity precursors of lanthanum carbonate, strontium carbonate, gallium oxide and magnesium oxide in appropriate stoichiometric ratios and calcining at a temperature of 1200°C for 4 hours in air. The calcined powders were lightly crushed using alumina mortar and pestle and the calcination step was repeated for completing the solid-state reaction. Electrode materials such as $La_{0.9}Sr_{0.1}MnO_3$ (LSM), $La_{0.6}Sr_{0.4}Co_{0.8}Fe_{0.2}O_3$ (LSCF), $Ce_{0.85}Gd_{0.15}O_2$ (GDC) and $Ce_{0.6}La_{0.4}O_2$ (LDC) were also made using the same mixing and calcination techniques. X-ray powder diffraction analysis confirmed the composition, phase and purity of the material. All the synthesized powders (LSGM, LSM, LSCF, GDC, LDC) and NiO powder purchased from Baker were then separately ball-milled in methanol. Laser Scattering Particle Size Distribution Analyzer (Horiba LA-910) was periodically used at different intervals of the ball milling process to determine the particle size and distribution. The ball milling process was stopped when the desired particle size and distribution were obtained.

Symmetrical cell fabrication: Calcined and milled LSGM powders at room temperature were die-pressed at 10000psi pressure into pellets and sintered in air at 1450°C for 4 hours. The sintered LSGM pellets were 1.4 mm thick and 2 cm in diameter. The LSGM pellets were then all finely ground to a uniform 1 mm thickness using diamond-grinding discs. LSM-LSGM, LSCF-LSGM, NiO-GDC, and NiO-LDC composite electrodes were prepared by thoroughly mixing desired amounts of the powders. The electrode powders (LSM, LSM-LSGM, LSCF, LSCF-LSGM, NiO-GDC, and NiO-LDC) were each dispersed in α-terpeniol solvent to form a paste. For the cathode electrodes (LSM, LSM-LSGM, LSCF, and LSCF-LSGM) and the anode without the buffer layer, the ground LSGM electrolyte pellets were masked with Scotch™ tape to form an outer ring on both sides and the electrode pastes were painted smoothly on the open circular surfaces. The painted LSGM electrolyte pellets were air-dried, masks removed and fired in air at elevated temperature for 2 hours. The firing temperature was 1100°C for all the cathodes and 1200-1300°C for the anodes (i.e. NiO-GDC and Ni-LDC electrode samples). All electrodes had the same effective area of around 1.33cm^2. When GDC or LDC buffer layers were employed between the Ni-doped-ceria composite anode and the LSGM electrolyte, very fine GDC or LDC powders were dispersed in α-terpeniol solvent to form a paste which was painted on both sides of the LSGM electrolyte. They were air dried and sintered at 1200-1300°C and the anodes were then applied following the procedure described earlier. For the cathode materials, two pieces of platinum mesh were co-sintered on both electrode surfaces to act as current collectors. Lead wires of Pt were used to connect the platinum-mesh current collectors to the measuring instrument. For the anode materials, pieces of nickel mesh were pressed over the electrode surfaces and co-sintered in a reducing atmosphere. Nickel lead wires were used to connect the nickel-mesh current collectors to the measuring instrument.

AC impedance characterization: The experimental setup using the symmetrical-cell arrangement is shown in Figure 1. In this setup, the symmetrical cell was exposed to the same oxidizing (cathodic), or reducing (anodic) atmosphere on both sides and a two-probe configuration was used to measure the impedance spectra. During measurement a constant flow rate of air was maintained for experiments involving the cathode materials,

and a constant flow rate of forming gas (95% argon-5% hydrogen) bubbled through water at 25^{o}C was maintained for experiments involving the anode materials. The measurements were made by applying a small-amplitude AC voltage (10mV) to the cell and monitoring the response current as a function of the AC frequency (from 1mHz to 65KHz). A plot of the imaginary part of the measured impedance versus the real part reveals details of the individual ohmic and polarization contributions to the total resistance of the cell. Impedance measurements were made in the temperature range of 600-800^{o}C in 50^{o}C increments for all the samples using a Perkin-Elmer potentiostat/galvanostat (model 263A) and Solartron analytical-frequency-response analyzer (model 1250).

The impedance measurements were performed both as a function of composition for the LSM-LSGM, Ni-GDC, and Ni-LDC electrodes and as a function of electrode thickness for the LSCF electrodes. After electrochemical testing, the samples were sectioned, epoxy mounted and polished. Optical microscopy and scanning electron microscopy were used to measure the grain size, porosity and thickness of the electrodes and confirm the consistency of the microstructure. Electron microprobe analysis and wavelength dispersive spectroscopy were also used to determine diffusion profiles of the elements at the interfaces.

Results and Discussions

Electrode Microstructures: The microstructure of the composite cathode and anode is crucial to achieving high power densities while operating the cell. Fine microstructure, fine connected porosity and well dispersed ionic and electronic conductors are essential for a good electrode exhibiting low charge-transfer or interfacial polarization. It has been theoretically shown by Tanner et al. [7,8] that the effective charge-transfer resistance scales as the square root of the grain size of the electrode material. However, there is a limit to the acceptable pore size. When the electrode pore size is comparable to the mean free path of the gases being transported in and out of the electrodes, the cell performance is dominated by concentration (mass-transfer) polarization. To achieve a balance between these two conflicting requirements, graded electrode structures with a finer microstructure and porosity close to the electrolyte and coarser microstructure and larger porosity away from it needs to be developed for the supporting electrode. For instance, for an anode-supported SOFC, the fine electrode microstructure close to the electrolyte would have a large three-phase-boundary (ionic-electronic-gas) length and facilitate charge-transfer reactions and the coarser microstructure and porosity of the thicker outer anode layer would facilitate gas transport. In this investigation we are focussing our attention on the fine microstructure that is needed at the electrode interface with the electrolyte.

Fractured surfaces of the LSM, LSM-LSGM, LSCF, LSCF-LSGM, Ni-GDC, and Ni-LDC electrodes and their interfaces with the electrolyte/barrier layer show that these electrodes have similar microstructures in terms of their interfacial adherence with the LSGM electrolyte, porosity and grain size. The grain size is on the order of 1-2 μm and the porosity is between 50-55% measured in terms of percentage area of the pore from the micrographs using Adobe Photoshop software. A sample, cross section of the fractured surface of the LSM-LSGM electrode/electrolyte interface along with the back-scattered electron image of the same interface is shown in Figure 2. Based on the grain size, porosity

and thickness (10-60μm) of the electrodes, gas diffusion is not expected to control the interfacial polarization process particularly for small applied potentials that were used for the AC impedance measurements.

Impedance spectroscopy: A typical impedance plot measured using the symmetrical cell arrangement is shown in Figure 3. For all samples measured in this investigation, a single depressed arc was observed. As discussed elsewhere by previous workers [9-11], the high-frequency intercept of the impedance spectrum gives the ohmic resistance of the cell (R_s), which includes the resistive contributions of the electrolyte, the two electrodes, the current collectors and the lead wires. The low-frequency intercept gives the total resistance ($R_s + R_p$), which includes the ohmic resistance of the cell, concentration polarization (or mass transfer polarization) resistance and the effective interfacial polarization resistance (R^{eff}_{redox}). The total polarization resistance of the electrode (R_p) is then extracted by subtracting the high-frequency intercept from the low-frequency intercept on the impedance plot. Given that the electrodes are thin, the amplitude of the applied AC voltage is small (10mV), and the gas flow over the electrode was continuous, it is most likely that the effective interfacial polarization resistance, R^{eff}_{redox}, dominates the polarization resistance for the electrodes, i.e. the concentration polarization is negligibly small and R_p is essentially equal to R^{eff}_{redox}.

Selection of Cathode Material: In order to lower the interfacial polarization it is well known that the electrode needs to be a mixed conductor (have both electronic and oxygen ion conductivities) [1,6]. Since, LSM is a p-type semi-conductor [1,3], it is advantageous to provide the oxygen ion conductivity by mixing it with LSGM. On the other hand, since the LSCF is already a mixed conductor [12,13], mixing it with LSGM is not expected to significantly lower the interfacial polarization. However, it is to be noted that there is a 50% mismatch in thermal expansion coefficient between the LSCF electrode material and LSGM electrolyte material [14,15]. Therefore from the point of view of lowering the interfacial thermal stresses it is desirable to have a LSCF-LSGM composite electrode as the cathode. To explore these concepts, several cathode materials, LSM, LSCF, LSM-LSGM and LSCF-LSGM composite electrodes were studied for possible application in Intermediate Temperature (IT)-SOFCs based on the LSGM electrolyte. Figure 4 shows a comparison of the polarization resistances of the above cathode materials as a function of temperature measured using impedance spectroscopy on symmetric cells as outlined earlier. The polarization resistance is plotted as inverse resistance versus inverse temperature. From these studies of cathode materials compatible with LSGM electrolyte it was determined that a 50 vol% LSCF-LSGM porous composite would serve as the best cathode material. As can be seen from Figure 4, the composite LSCF-LSGM cathode has an interfacial polarization resistance that is several orders of magnitude lower than the LSM-LSGM composite cathode, although as expected the later is lower than the conventional single-phase LSM electrode. The interfacial polarization resistance of the LSCF-LSGM composite cathode is also slightly lower than the single phase LSCF cathode. In addition, considering the thermal expansion coefficient (TEC) mismatch between the LSCF cathode and LSGM electrolyte, the LSCF-LSGM composite will also be preferred over the single phase LSCF material. Our investigations of mixed-conducting cathode materials have also revealed a dependence of polarization resistance on electrode thickness. The polarization resistance of LSCF cathode on LSGM electrolyte is shown in Figure 5 as a function of thickness. The polarization of the cathode layer initially decreases

sharply with increasing electrode thickness and then levels off asymptotically. The initial decrease of the cathode polarization resistance can be rationalized on the premise that increasing the electrode thickness results in an increase in the number of electrochemical reaction sites, i.e. total three-phase boundary length in the case of composite cathodes, or total pore area in the case of mixed ionic-electronic conductors. The subsequent leveling off of the polarization resistance is due to the fact that above a certain critical electrode thickness the migration of the oxygen ions from the reaction sites to the electrode/electrolyte interface become rate controlling. Thus, there is a certain critical thickness beyond which the cathodic polarization resistance shows no further decrease with increasing thickness. This critical electrode thickness has been shown to be a strong function of the microstructure (grain size) and porosity [7,8], i.e. finer the microstructure and finer the porosity, smaller the critical thickness. Based on our cathode microstructure, it is clear that a thickness of 40 μm is sufficient to minimize the interfacial polarization resistance.

Selection of Anode Material: Nickel is a well-known SOFC anode material, and acts as the fuel side electrocatalyst and current collector. GDC is an excellent oxygen-ion conductor, is chemically and mechanically compatible with the LSGM electrolyte and has electronic conductivity under reducing conditions [1,14,16]. Therefore, Ni-GDC cermet is expected to be an effective anode if its reaction with the LSGM electrolyte can be prevented. The reactivity of the Ni-GDC cermet anode with the LSGM electrolyte was studied by using the Ni-GDC/LSGM/Ni-GDC symmetrical cell at 800^{o}C under a reducing atmosphere (H_2-bubbled through 25^{o}C water bath). Both the ohmic and interfacial polarization resistances increased gradually with time, which is shown in Figure 6. These results were used to confirm that this was due to Ni reacting with the LSGM and forming insulating phases (lanthanum nickelates) at elevated temperatures [17]. Therefore the use of a layer of doped ceria between the LSGM electrolyte and Ni-GDC anode to prevent direct contact between the Ni in the anode with the lanthanum in the LSGM electrolyte was explored.

Ni-GDC electrodes with GDC buffer layer on LSGM electrolyte: It was apparent from the wavelength-dispersive-spectroscopy (WDS) analysis of these samples that the GDC barrier layer allowed lanthanum diffusion from the LSGM electrolytes (Figure 7). Lanthanum diffusion from LSGM into GDC leads to the formation of $Ce_{1-x-y}La_xGd_yO_2$ solution in the GDC buffer layer and resistive phases $LaSrLa_3O_7$ or $LaSrGaO_4$ at the LSGM electrolyte interface [18]. The latter significantly increases the ohmic resistance of the cell. By decreasing the sintering temperature of the GDC buffer layer it is possible to decrease the lanthanum diffusion, but this leads to incomplete densification and poor interfacial adherence of the GDC buffer layer to the LSGM electrolyte. This also causes penetration of the Ni-GDC anode slurry into the LSGM electrolyte surface through the porous GDC buffer layer. This results in a time-dependent increase of interfacial polarization similar to when the GDC buffer layer was absent. In conclusion, it was determined that the GDC layer did not serve as an effective buffer layer between the LSGM electrolyte and the Ni-GDC composite anode.

Ni-GDC and Ni-LDC electrodes with LDC buffer layer on LSGM electrolyte: Next, lanthanum doped ceria (LDC) was employed as the barrier layer between the LSGM electrolyte and the Ni-composite anode in order to limit or eliminate lanthanum diffusion from the LSGM electrolyte into the barrier layer. The idea was to eliminate the lanthanum

chemical potential gradient at the interface that results in lanthanum diffusion. It is to be noted that unlike the LSGM electrolyte which has a perovskite phase, the LDC barrier layer has a fluorite structure. The Ni in the anode is not expected to react with the lanthanum in the LDC barrier layer as long as the La content in the LDC is below 50mole% in the cationic site [19]. It was observed that, unlike the GDC, when the LDC barrier layer had 40 mole% La in the Ce site and was sintered at 1300^{o}C, there was no detectable La diffusion from the LSGM electrolyte. The 40mol% Lanthanum doped ceria (LDC) likely has the same La chemical potential as in the LSGM and therefore prevented the La diffusion between LSGM electrolyte and the LDC buffer layer [19,20]. Also since the La content was below 50mole%, it was expected to be stable in contact with the Ni-composite anode. Since LDC was being employed as the barrier layer, it was logical to also investigate Ni-LDC composite along with the Ni-GDC composite anodes. The temperature dependence of the interfacial polarization resistance for Ni-LDC and Ni-GDC (70 v% Ni) composite anode sintered at 1300^{o}C over the LDC barrier layer that was also sintered at 1300^{o}C is shown in Figure 8. As can be seen from Figure 8, the Ni-GDC electrode has a smaller interfacial polarization resistance than the Ni-LDC electrode, especially at lower testing temperatures, i.e. 600-700^{o}C. At higher testing temperature, i.e. 700-800^{o}C, the polarization resistances of both electrodes approached one another. As discussed earlier, by increasing the conductivity of the ionic conducting phase in the composite electrode it is possible to lower the interfacial polarization resistance. GDC has a higher ionic conductivity compared to LDC [21], especially at lower temperatures, and therefore the Ni-GDC composite anode has a lower polarization resistance than the Ni-LDC electrode. In order to compare between the effectiveness of the GDC and the LDC barrier layers, the total resistance is plotted as a function of temperature in Figure 9 for the two symmetrical cells with Ni-GDC (70 v% Ni) composite anode but each having a different barrier layer sintered at 1300^{o}C; GDC and LDC. It is clear from this figure that given identical dimensions of the LSGM electrolyte, the barrier layers and the anodes, the lanthanum diffusion from the LSGM electrolyte with the GDC barrier layer causes the total resistance of the symmetrical cell to be significantly higher than the corresponding cell with the LDC barrier layer.

Time dependence of the interfacial polarization resistance at 800^{o}C of the LSGM symmetrical cells with Ni-LDC and Ni-GDC (70 v% Ni) composite electrodes with LDC buffer layer is shown in Figure 10. Also shown in the same figure is the interfacial polarization resistance of the Ni-GDC (70 v% Ni) composite electrode without the buffer layer. The interfacial polarization resistances of both Ni-LDC and Ni-GDC electrodes with LDC buffer layer were stable over a period of two weeks, whereas the interfacial polarization resistance of the Ni-GDC electrode without the LDC buffer layer increased continuously with time due to the reaction between Ni and the lanthanum in the LSGM electrolyte.

Effect of Ni-LDC and Ni-GDC electrode composition on interfacial polarization resistance: The temperature dependence of the interfacial polarization resistance for symmetrical cells with LSGM electrolyte and Ni-LDC and Ni-GDC (50 or 70 v% Ni) composite electrodes sintered at 1300^{o}C over the LDC buffer layer (sintered at 1300^{o}C) is shown in Figure 11. As discussed earlier, the Ni-LDC (70 v% Ni) electrode has the largest interfacial polarization resistance, while all other electrodes, i.e. Ni-LDC5050 (50 v% Ni), Ni-GDC7030 (70 v% Ni), and Ni-GDC5050 (50 v% Ni), had almost the same interfacial

polarization resistance. Moreover, for Ni-LDC5050, Ni-GDC7030 and Ni-GDC5050 electrodes, the polarization resistance did not decrease much when the testing temperature was increased from 600°C to 800°C. This meant that from the point of view chemical reactivity and thermal expansion coefficients it would be preferable to select Ni-LDC5050 as the composite anode for the LSGM electrolyte with the LDC barrier layer.

Materials System for the Intermediate Temperature Solid Oxide Fuel Cell:

Based on this investigation the desirable materials system for the Intermediate-Temperature Solid Oxide fuel Cell based on the LSGM electrolyte will consist of:

(a) 50% by volume of LSCF-LSGM composite cathode having a fine microstructure (1-2μm grains), porosity of 40-50% and thickness of at least 30-40μm.

(b) a dense adherent barrier layer (5μm) of lanthanum doped ceria (LDC) between the LSGM electrolyte and the anode.

(c) 50% by volume of Ni-LDC composite anode having a fine microstructure near the LDC buffer layer and coarser microstructure away from the buffer layer; porosity 40-50%. Since the design is based on an anode-supported cell, the anode can be 1-2 mm thick and the fine microstructure region at least 30-40μm.

The desired cell structure is schematically shown in Figure 12.

Conclusions

The materials system investigated for the Intermediate-Temperature (600-800°C) SOFC is based on the LSGM electrolyte. Electrode materials were investigated by using impedance spectroscopy on symmetrical cells. Among the cathode materials (LSM, LSM-LSGM, LSCF and LSCF-LSGM), pure LSM electrode has the worst interfacial polarization resistance. The addition of LSGM electrolyte material to the LSM electrode increases the mixed-conducting boundary with the gas phase and lowers the interfacial polarization resistance. Mixed-conducting LSCF electrode however, has much lower polarization resistance compared to the LSM-LSGM composite electrodes. Although adding LSGM electrolyte material to the LSCF electrode doesn't improve the electrode performance very much, it can buffer the larger thermal expansion coefficient of LSCF compared to the LSGM electrolyte. The polarization resistance of the LSCF electrode decreased asymptotically as the electrode thickness increased. The optimum electrode thickness for the given microstructure was determined to be 30-40μm. As Ni in the anode material reacts with La in the LSGM electrolyte it increases the interfacial polarization resistance. A buffer layer between the LSGM electrolyte and Ni-GDC anode is necessary to prevent this reaction. However, if the buffer layer is GDC, La diffusion occurs from the LSGM electrolyte. LDC appeared to serve as an effective buffer layer between the LSGM electrolyte and the Ni-composite anode. Polarization resistance of several Ni-GDC and Ni-LDC composite anodes with LSGM electrolyte and LDC buffer layer sintered at 1300°C were also investigated. Ni-LDC (70 v% Ni) electrode has the largest interfacial polarization resistance, while all other electrodes, i.e. Ni-LDC (50 v% Ni), Ni-GDC (70 v% Ni), and Ni-GDC (50 v% Ni), had almost the same interfacial polarization resistance. From the point of view chemical reactivity and thermal expansion coefficients it would be preferable to select Ni-LDC as the composite anode for the LSGM electrolyte with a thin LDC barrier layer.

References

1) N. Q. Minh and T. Takahashi, *Science and Technology of Ceramic Fuel Cells*, Elsevier Publishing Company Inc., New York, (1995).
2) B.C.H. Steele, *Solid State Ionics*, **75**,157 (1995).
3) N. Q. Minh, *J. Am. Ceram. Soc*., **76**, 563 (1993).
4) M.Feng, and J. B. Goodenough, *Eur. J. Solid State Inorg. Chem*., **31**, 663 (1994).
5) B. C. H. Steele, *Solid State Ionics*, **129**, 95 (2000).
6) M. T. Colomer, B. C. H. Steele and J. A. Kilner, *Solid State Ionics*, **147**, 41 (2002).
7) C.W. Tanner, K.Z. Fung and A.V. Virkar, *J. Electrochem. Soc.,* **144**, 21 (1997).
8) A.V. Virkar, J.Chen, C.W. Tanner and J.W. Kim, *Solid State Ionics,* **131** 189 (2000).
9) H. Hu and M. Liu, *Solid State Ionics*, **109**, 259 (1998).
10) S. Wang, X. Lu and M. Liu, *J. of Solid State Electrochemistry*, **6**, 384 (2002).
11) J. R. Macdonald, *Impedance Spectroscopy: Emphasizing Solid Materials and Systems*, Wiley, New York, (1987).
12) L. W. Tai, M. M. Nasrallah, H. U. Anderson, D. M. Sparlin and S. R. Sehlin, *Solid State Ionics*, **76**, 259 (1995)
13) L. W. Tai, M. M. Nasrallah, H. U. Anderson, D. M. Sparlin and S. R. Sehlin, *Solid State Ionics*, **76**, 273 (1995).
14) H. Hayashi, M. Suzuki, and H. Inaba, *Solid State Ionics*, **128**, 131 (2000).
15) A. Petric, P. Huang, and F. Tietz, *Solid State Ionics*, **135**, 719, (2000).
16) S. Sameshima, T. Ichikawa, M. Kawaminami, and Y. Hirata, *Materials Chemistry and Physics*, **61**, 31 (1999).
17) X. Zhang, S. Ohara, R. Maric, H. Okawa, T. Fukui, H. Yoshida, T. Inagaki, and K. Miura, *Solid State Ionics*, **133**, 153 (2000).
18) M. Hrovat, A. Ahmad-Khanlou, Z. Samardž ija, and J. Holc, *Materials Research Bulletin*, **34**, 2027-2034 (1999).
19) K. Huang, J. H. Wan, and J. B. Goodenough, *J. Electrochem. Soc.*, **148**, A788 (2001).
20) Y. Matsuzaki and I. Yasuda, *Solid State Ionics*, 152-153, 463 (2002).
21) M. Mogensen, T. Lindegaard, U. R. Hansen, in *Ionic and Mixed Conducting Ceramics*, T.A.Ramanarayanan, W.L.Worrel and H.L. Tuller, Editors, P.448. The Electrochemical Society Proceedings Series, Pennington, NJ (1994).

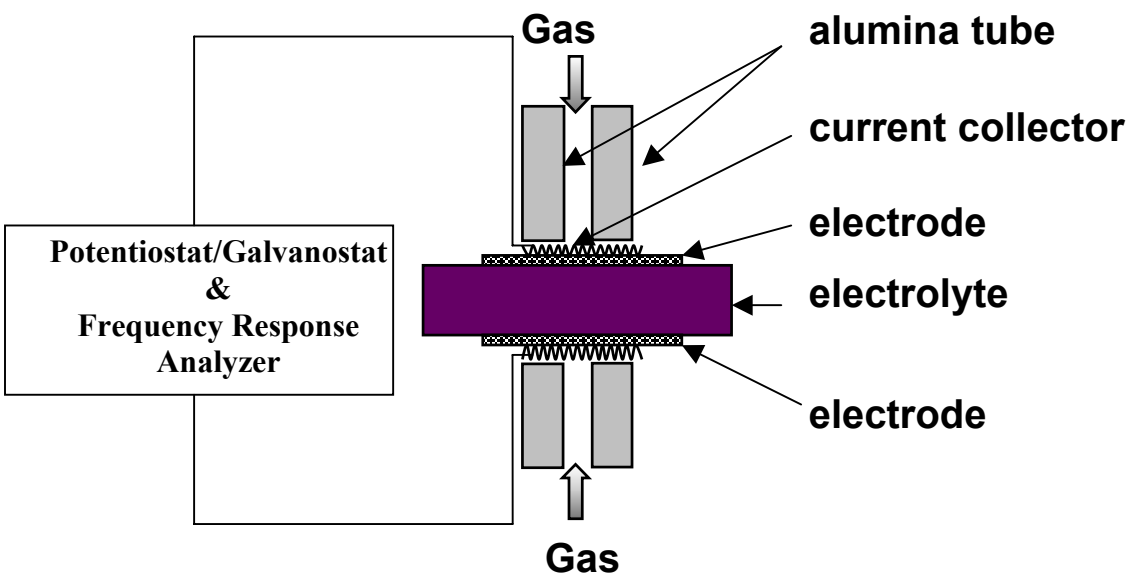

Figure 1. A schematic diagram showing the experimental setup of symmetrical cells for impedance measurements.

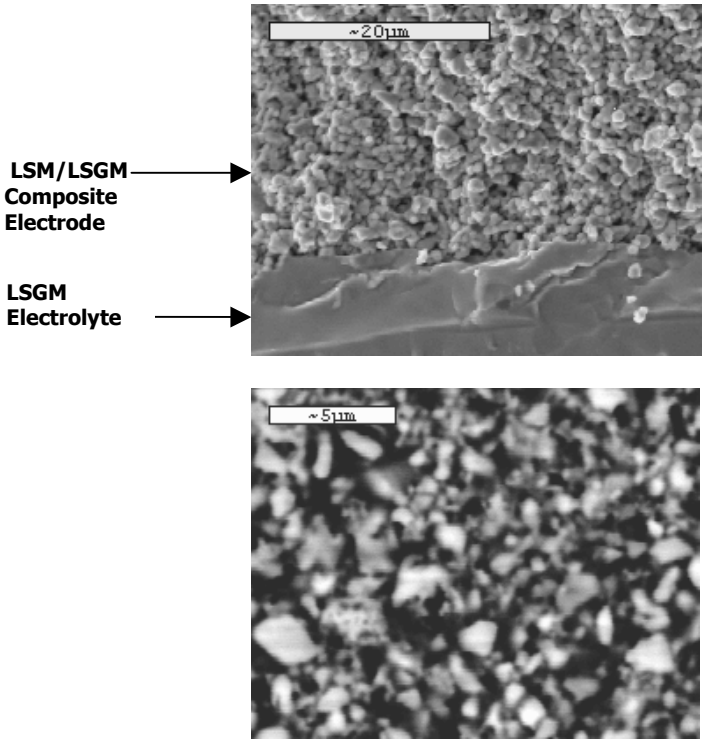

a

b

Figure 2. (a) SEM micrographs of fracture surfaces of LSM/LSGM interface, and (b)back-scattered-SEM micrograph of the polished surfaces of the same electrode.

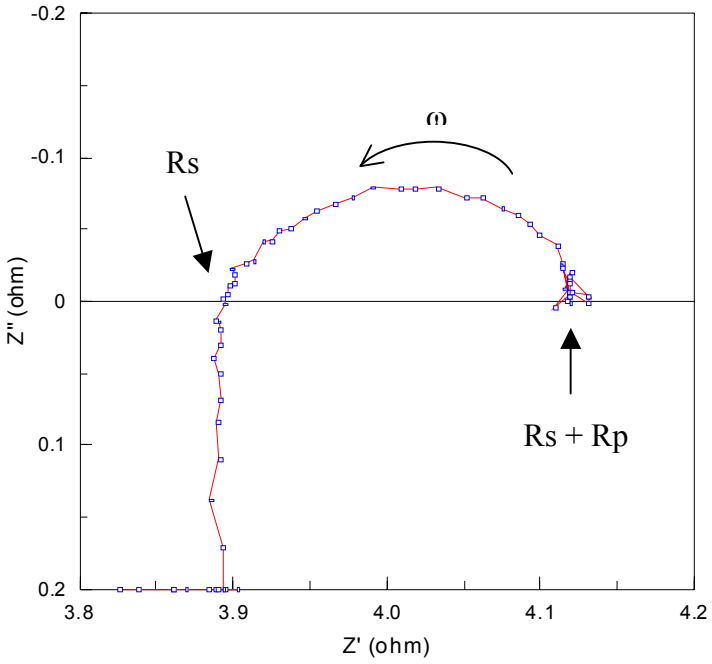

Figure 3

Figure 3. A typical impedance plot of an LSGM symmetrical cell with identical electrodes (cathode/anode) at 800°C.

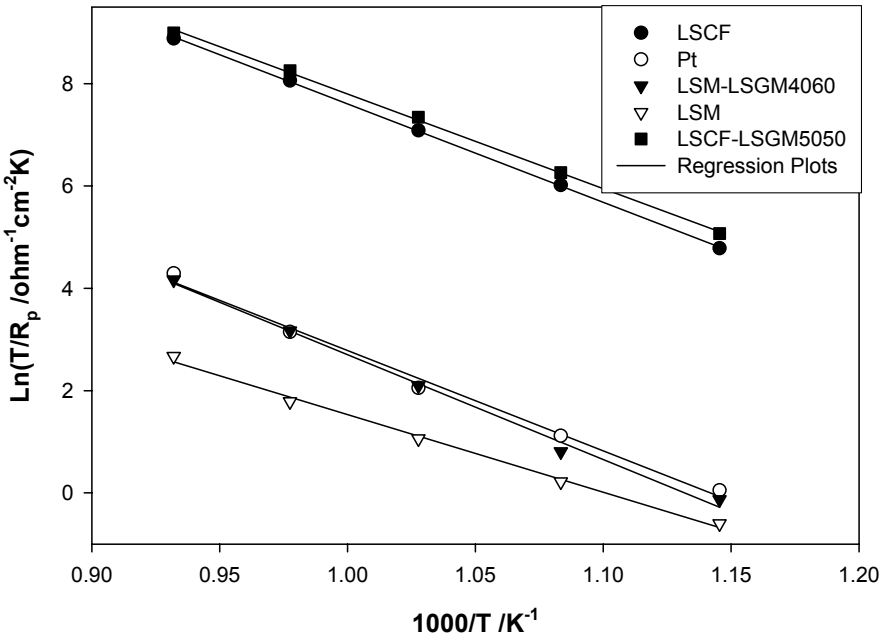

Figure 4. Comparison of interfacial polarization resistances of various cathode materials on LSGM electrolyte.

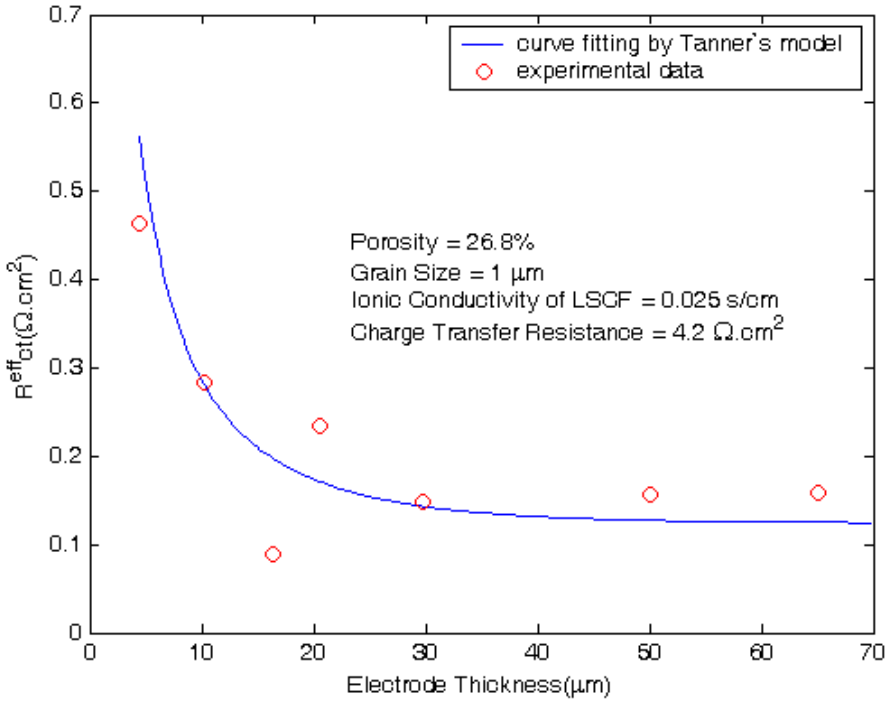

Figure 5. Variation of LSCF interfacial polarization resistance over LSGM electrolyte as a function of thickness at 800 ^{0}C.

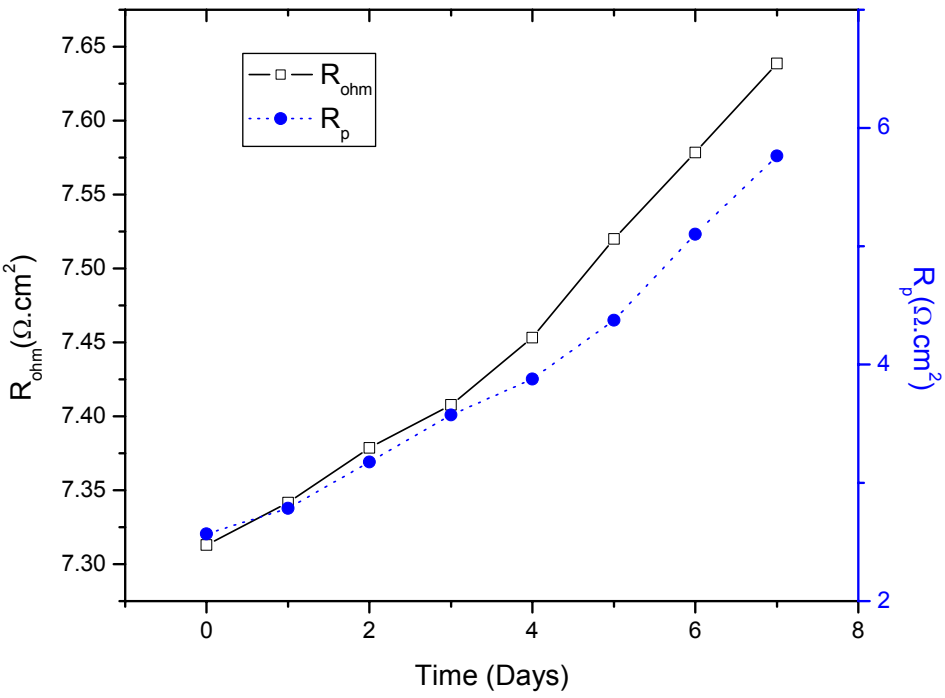

Figure 6. Time dependence of ohmic and polarization resistances of symmetrical Ni-GDC/LSGM/Ni-GDC cell measured in reducing atmosphere at 800^{o}C.

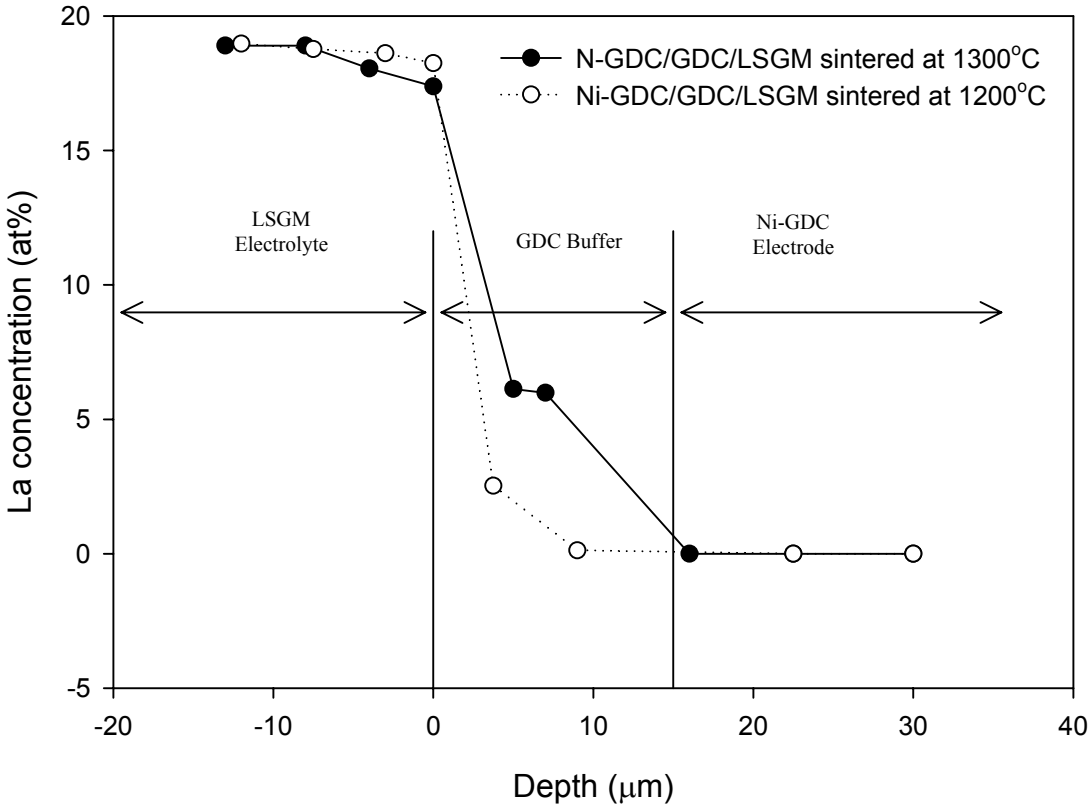

Figure 7. Diffusion profile of lanthanum in the GDC buffer layer.

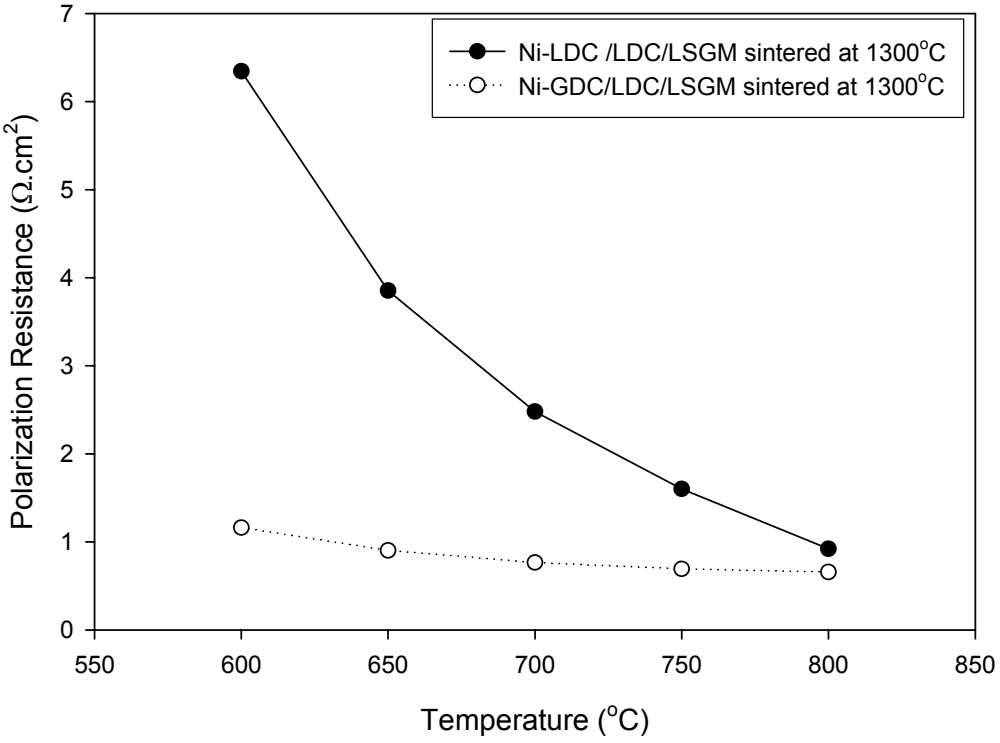

Figure 8. Comparison of the effect of the dopant in ceria in the composite Ni electrodes on the interfacial polarization resistance as a function of temperature.

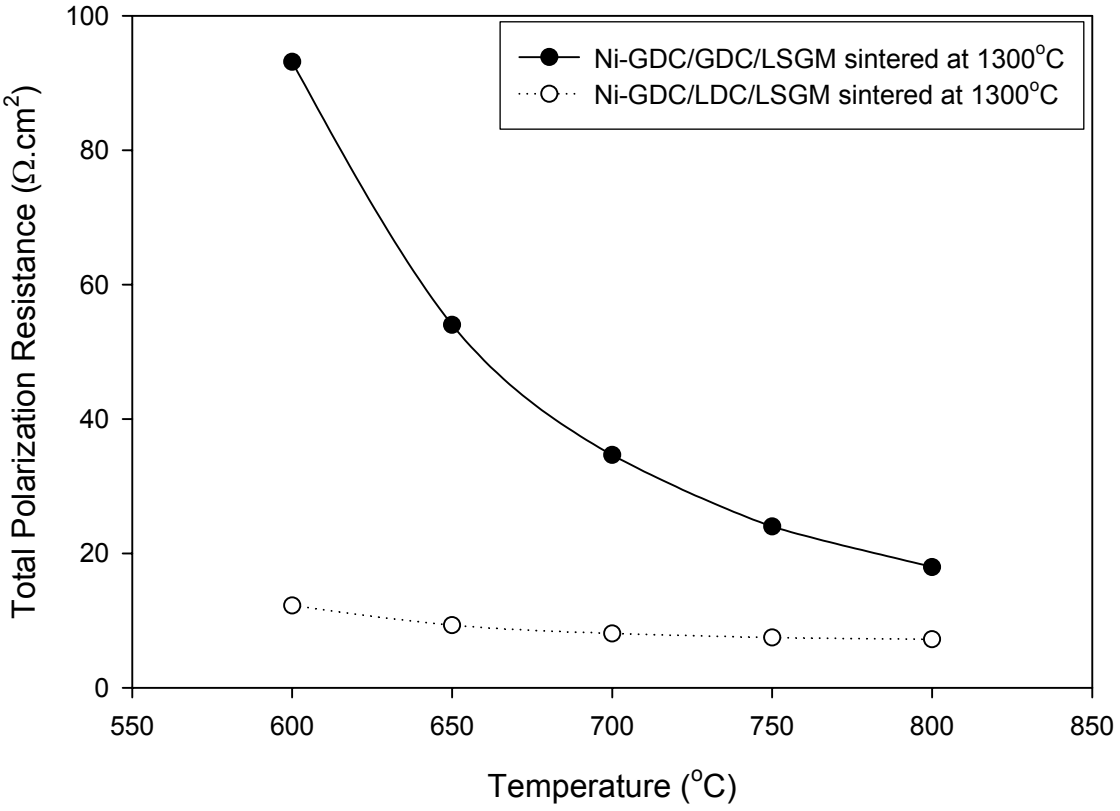

Figure 9. Comparison of the effect of GDC and the LDC barrier layers on the total cell resistance of the symmetrical cells with Ni-GDC composite electrodes as a function of temperature.

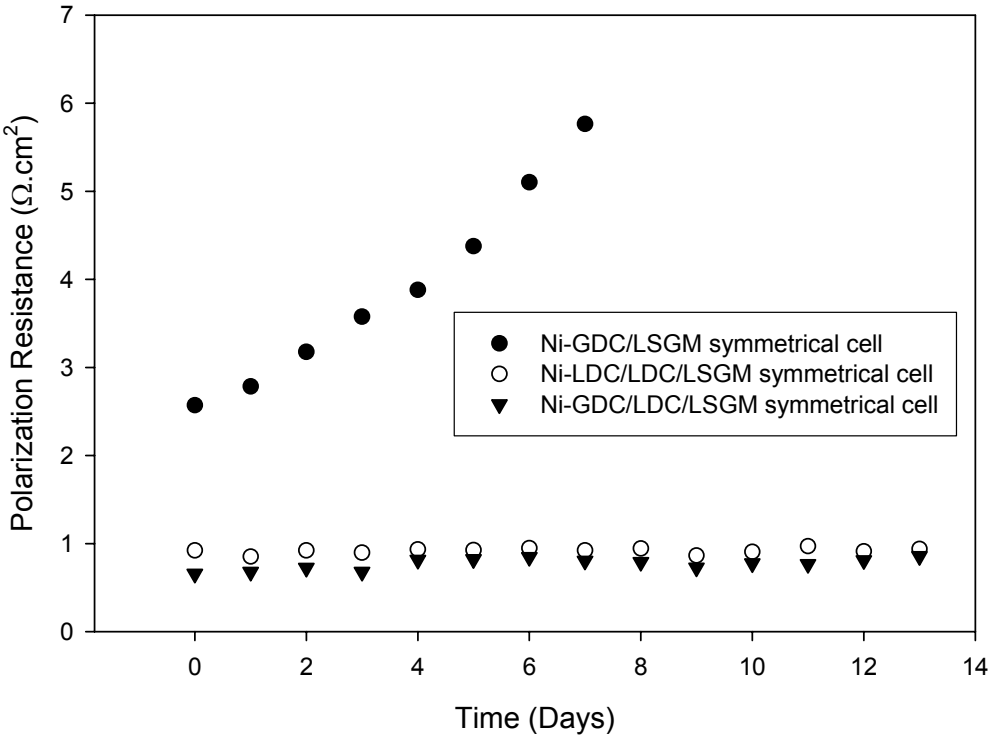

Figure 10. Time dependence of the interfacial polarization resistances of cermet anodes with and without the LDC barrier layer over LSGM electrolyte at 800^{o}C.

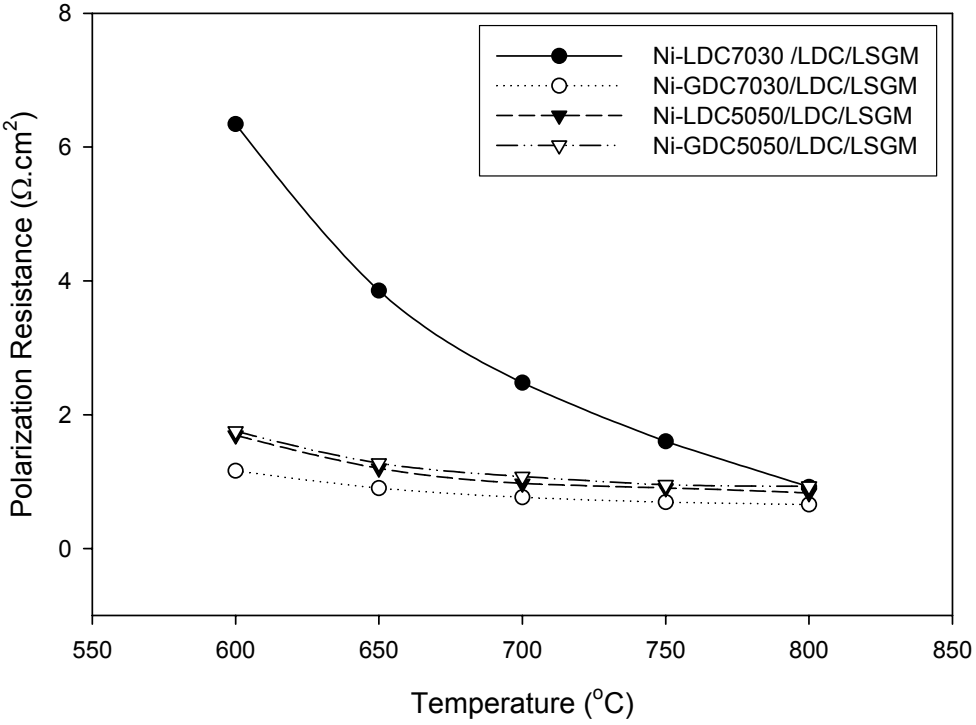

Figure 11. Comparison of the effect of the composition of the Ni-doped ceria composite electrodes on the interfacial polarization resistance as a function of temperature.

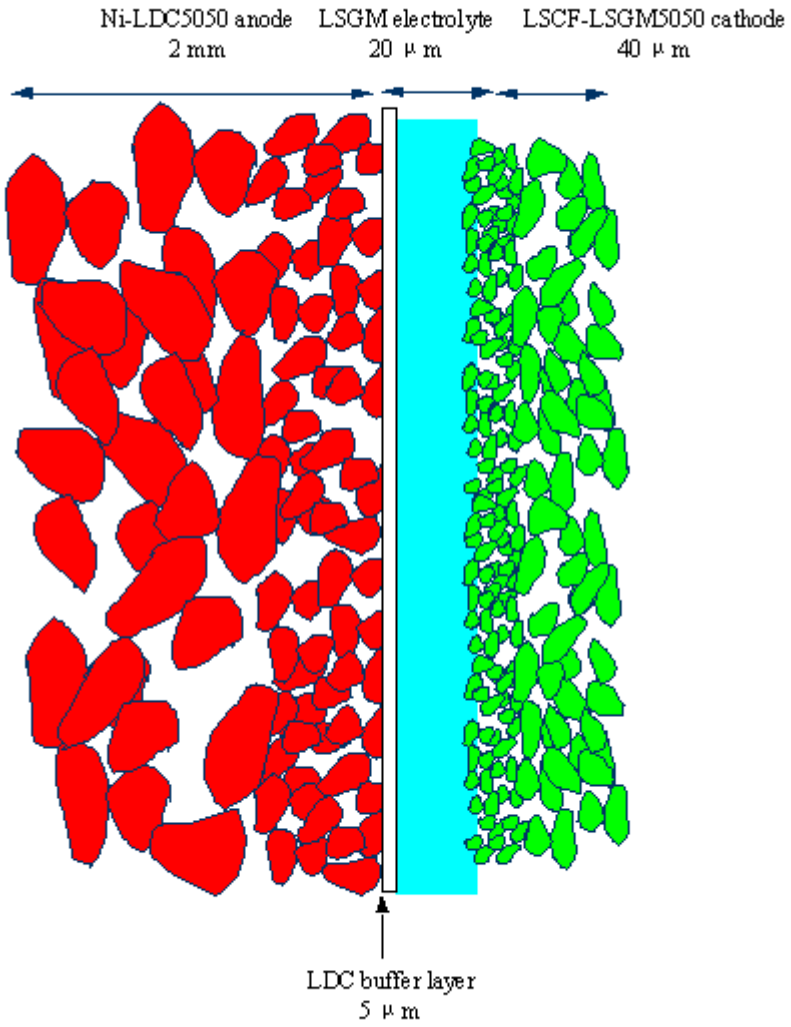

Figure 12. Schematic of an anode supported Intermediate Temperature Solid Oxide Fuel Cell based on LSGM electrolyte.